Evolution Characteristics of Multi-Source Mechanical Responses in Soft-Hard Interbedded Tunnel Surrounding Rock with Different Bedding Dip Angles

Xiaohui Wang*
Xi'an-Chengdu Passenger Dedicated Line Shaanxi Co., Ltd., Xi'an, China
**Corresponding Author*

Abstract: To clarify how bedding orientation affects the excavation stability of tunnels constructed in soft-hard interbedded rock masses, a series of three-dimensional numerical models with different bedding dip angles were developed using 3DEC. The excavation-induced response of the surrounding rock was evaluated by jointly examining the vertical displacement field, vertical stress redistribution, and plastic-zone development. The results show that the vertical displacement field, vertical stress field, and plastic zone are approximately symmetric at bedding dip angles of 0° and 90°. By contrast, pronounced asymmetric responses occur at dip angles of 30°~60°, with the zones of large vertical displacement, vertical stress concentration, and plastic deformation migrating preferentially along the bedding direction. As the bedding dip angle increases, the vertical deformation of the surrounding rock decreases overall, accompanied by a progressive reduction in the peak vertical stress. Plastic failure is predominantly initiated and propagated along the bedding interfaces, indicating that both the failure path and the associated instability mode are strongly governed by bedding orientation.

Keywords: Tunnel; Soft-Hard Interbedded Surrounding Rock; Bedding Dip Angle; Numerical Simulation; Evolution Characteristics of Multi-Source Mechanical Responses.

1. Introduction

Sedimentary formations account for approximately 77.3% of China's land area, and tunnel construction therefore frequently encounters distinctly layered rock masses [1-3]. Owing to the widespread presence of bedding planes, joints, and other discontinuities, layered rock masses exhibit pronounced anisotropy and failure characteristics that differ markedly from those of homogeneous media [4-6]. In soft-hard interbedded strata, mechanical contrasts between adjacent layers and the controlling effect of structural interfaces further intensify nonuniform deformation and local instability after excavation. Investigating the excavation response of such tunnels under different bedding dip angles is therefore essential for clarifying their deformation and failure mechanisms, improving support design, and ensuring long-term tunnel stability.

Extensive investigations have been conducted on the stability of tunnels excavated in layered and soft-hard interbedded rock masses. Based on field monitoring and numerical analyses of the Yangjiaping Tunnel, Li et al. [7] found that the surrounding rock exhibited an overall inward squeezing response, with horizontal convergence considerably exceeding crown settlement. Ren et al. [8] employed ANSYS to evaluate the stability of a Grade V sandstone-mudstone interbedded section of the Simian Mountain Tunnel in Chongqing and subsequently optimized the primary support system. Taking the Tongmashan Tunnel as a case study, Tu [9] examined the instability process of horizontally bedded sandy slate and showed that progressive reductions in the strength of both the intact rock and bedding interfaces caused the failure mode to evolve from minor localized damage at the sidewalls to large-scale deformation of the entire opening. Ding et al. [10] used the discrete-element code PFC2D to simulate the Yong'an Tunnel and systematically compared the failure characteristics of the surrounding rock under different bedding dip angles. Their results indicated that both the proportion of exposed weak rock and the bedding inclination were major factors governing the resulting failure pattern. Vitali et al. [11] numerically investigated tunnel excavation under dip and against-dip configurations of discontinuities and clarified the mechanisms associated with the relative orientation between excavation direction and structural planes. Based on a highway tunnel project, Huang [12] analyzed the responses of representative points in the surrounding rock under different layer thicknesses and soft-to-hard layer thickness ratios.

Previous studies have investigated the deformation and failure of tunnels in layered rock masses through field monitoring, numerical simulation, and physical model testing. However, the coupled effects of bedding dip angle and mechanical contrasts between adjacent rock layers remain insufficiently understood. In this study, 3DEC models with different bedding dip angles are established, and the excavation response of soft-hard interbedded surrounding rock is evaluated in terms of vertical displacement, vertical stress redistribution, and plastic-zone development. The results are intended to improve the understanding of bedding-controlled deformation and failure and to support stability assessment in complex layered geological conditions.

2. Numerical Modeling Scheme for Tunnel Excavation in Soft-hard Interbedded Surrounding Rock

2.1 Numerical Model Construction and Boundary Conditions

To investigate the influence of bedding dip angle on the excavation response of tunnels in soft-hard interbedded surrounding rock under high geo-stress conditions, a numerical model was established using 3DEC. The model dimensions were set as 40 m × 40 m × 10 m. The surrounding rock was composed of alternating soft and hard rock layers, with a thickness ratio of soft rock to hard rock of 0.25. Specifically, the thicknesses of the soft and hard layers were 0.5 m and 2.0 m, respectively. Five bedding dip angles, namely θ = 0°, 30°, 45°, 60°, and 90°, were considered. The outer boundary of the model was discretized using a coarse mesh size of 2 m, while the region around the tunnel was refined to a mesh size of 0.5 m. The tunnel cross-section was designed as a straight-wall arch, with a clear width of 5m and a total height of 4.7 m. The crown was represented by a circular arc with a radius of 2.5 m, and the height of the straight-wall section was 2.2 m. The final numerical model is shown in Figure 1.

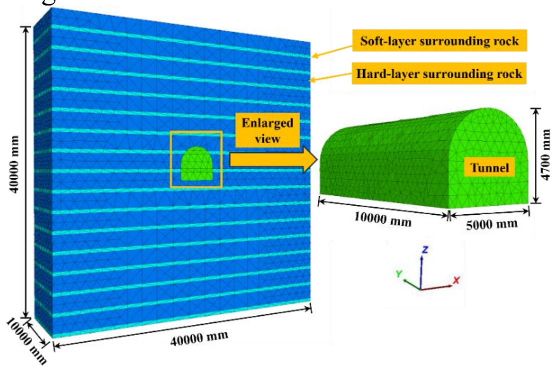

Figure 1. Numerical Model

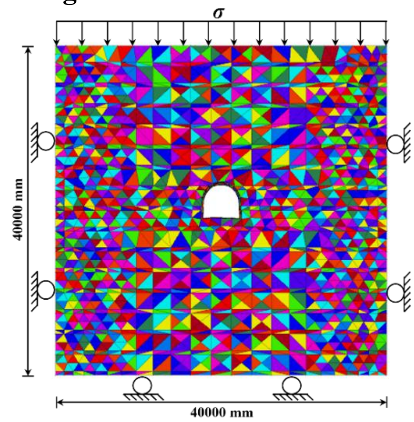

Figure 2. Boundary Conditions

As illustrated in Figure 2, a vertical stress of 26 MPa (σv) was applied to the upper boundary to represent the vertical in-situ stress under high-stress conditions. The bottom boundary was fully fixed, whereas normal displacements were constrained on the four lateral boundaries. Based on the prescribed in-situ stress ratios of σh/σH = 0.8 and σH/σv = 1.2, the minimum horizontal principal stress parallel to the tunnel axis and the maximum horizontal principal stress perpendicular to the tunnel axis were set to σh = 24.96 MPa and σH = 31.2 MPa, respectively. The hard-rock layers were assigned an elastic modulus of 25 GPa, cohesion of 2.40 MPa, internal friction angle of 35°, tensile strength of 2.00 MPa, Poisson's ratio of 0.30, and density of 2.65 g/cm³. The corresponding parameters for the soft-rock layers were 10 GPa, 1.10 MPa, 20°, 1.20 MPa, 0.36, and 2.80 g/cm³, respectively. For the bedding interfaces, the normal and shear stiffnesses were specified as 5.8 and 2.9 GPa/m, respectively, while the internal friction angle was set to 18°. Both the cohesion and tensile strength of the interfaces were taken as 1.0 MPa.

2.2 Excavation Process Simulation and Case Setup

To investigate the excavation-induced mechanical response of tunnels in soft-hard interbedded rock masses with different bedding dip angles, the initial in-situ stress field was first brought to equilibrium, after which the rock mass enclosed by the tunnel profile was removed to simulate excavation. The excavation process causes stress release and redistribution in the surrounding rock, thereby inducing deformation and localized plastic failure. During the calculation, the built-in functions of 3DEC were used to simultaneously track multiple response indicators around the tunnel cross-section, including the vertical displacement field, vertical stress field, and plastic-zone development.

Five representative bedding configurations, with dip angles of θ = 0°,30°,45°,60°, and 90°, were considered, as illustrated in Figure 3. To ensure direct comparability among the numerical cases, all parameters other than the bedding dip angle-including the model dimensions, boundary conditions, in-situ stress state, mechanical properties of the rock blocks, and bedding-interface parameters-were kept unchanged. Following tunnel excavation, the vertical displacement field, vertical stress field, and plastic-zone distribution were extracted for each case. The influence of bedding orientation on the excavation response of the soft-hard interbedded surrounding rock was subsequently evaluated by comparing the variations in peak response values and their spatial distribution patterns.

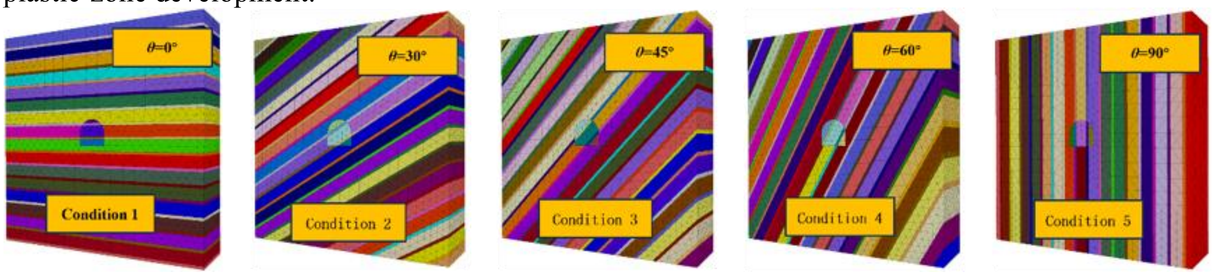

Figure 3. Excavation Simulation Scheme for Different Bedding Dip Angles

3. Evolution Characteristics of Multi-source Mechanical Responses in Soft-hard Interbedded Surrounding Rock with Different Bedding Dip Angles

3.1 Evolution of the Vertical Displacement Field

Numerical simulations were conducted for five representative cases with bedding dip angles of θ = 0°, 30°, 45°, 60°, and 90° to systematically investigate the influence of bedding orientation on the excavation stability of tunnels in soft-hard interbedded surrounding rock. The displacement field on the tunnel face cross-section indicates that the displacement distribution of the surrounding rock varies significantly under different bedding dip conditions.

The vertical displacement contours presented in Figure 4 reveal the following characteristics. (1) Excavation-induced vertical deformation is primarily concentrated around the crown and invert. Owing to the combined effects of the vertical in-situ stress and excavation unloading, crown settlement is greater than invert heave, and the displacement magnitude increases toward the tunnel opening. (2) The bedding dip angle exerts a pronounced influence on the spatial distribution of vertical displacement. At θ = 0° and 90°, the vertical displacement field is approximately symmetric. In contrast, at θ = 30°~60°, the high-displacement zones migrate preferentially along the bedding direction. Specifically, the zone of pronounced crown settlement shifts toward the right spandrel, whereas the region of invert heave extends toward the left wall foot. These observations indicate that inclined bedding interfaces provide a preferential path for deformation within the soft-hard interbedded rock mass. (3) As θ increases from 0° to 90°, the extent of the concentrated vertical displacement zone gradually decreases. The maximum crown settlement decreases from 95.26 mm at θ = 0° to 65.05 mm at θ = 90°, corresponding to a reduction of 31.71%. When θ ≤ 30°, the high-displacement zone above the crown extends to the model boundary; at larger dip angles, it becomes progressively confined to the vicinity of the tunnel.

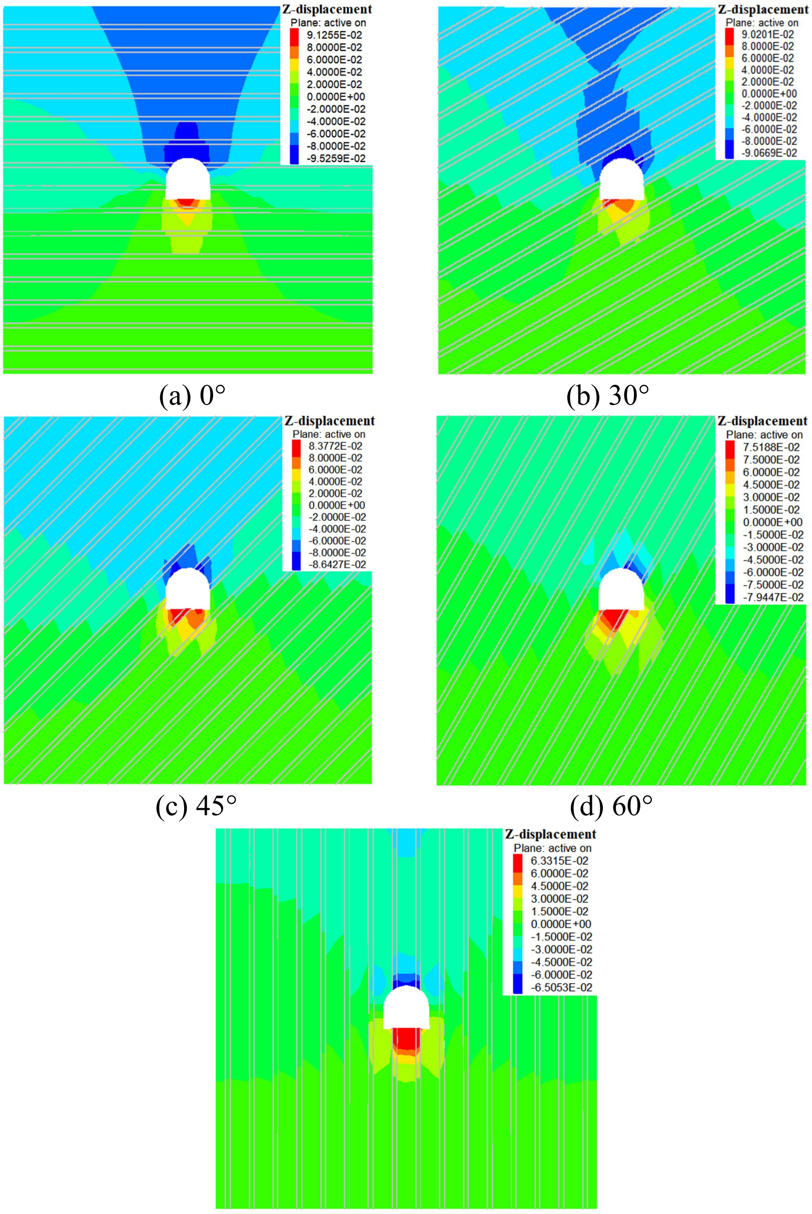

(a) 0° (b) 30°

(c) 45° (d) 60°

(e) 90°

Figure 4. Vertical Displacement Contours of the Surrounding Rock with DifferentBedding Dip Angles (unit: M)

3.2 Evolution of the Vertical Stress Field

The numerical results indicate that variations in bedding dip angle significantly affect the stress concentration and stress redistribution characteristics of soft-hard interbedded surrounding rock after excavation. As shown in the vertical stress contours in Figure 5, the following features can be observed. (1) All stress values are negative, indicating that the tunnel surrounding rock remains in a compressive stress state. After excavation unloading, obvious stress redistribution occurs around the tunnel. The closer the location is to the tunnel center, the more pronounced the stress variation becomes; conversely, the farther it is from the tunnel center, the closer the stress approaches the initial in-situ stress state. (2) When θ = 0° and 90°, the vertical stress field of the surrounding rock is generally symmetric. In contrast, when θ = 30°~60°, the high-stress zones extend asymmetrically along the bedding direction, indicating that inclined bedding planes have a strong controlling effect on the vertical stress transfer path of the surrounding rock. (3) With increasing θ, the extreme value of vertical stress continuously decreases. The peak vertical stress is 7.02 MPa at θ = 0° and decreases to 4.34 MPa at θ = 90°, corresponding to a reduction of 38.18%.

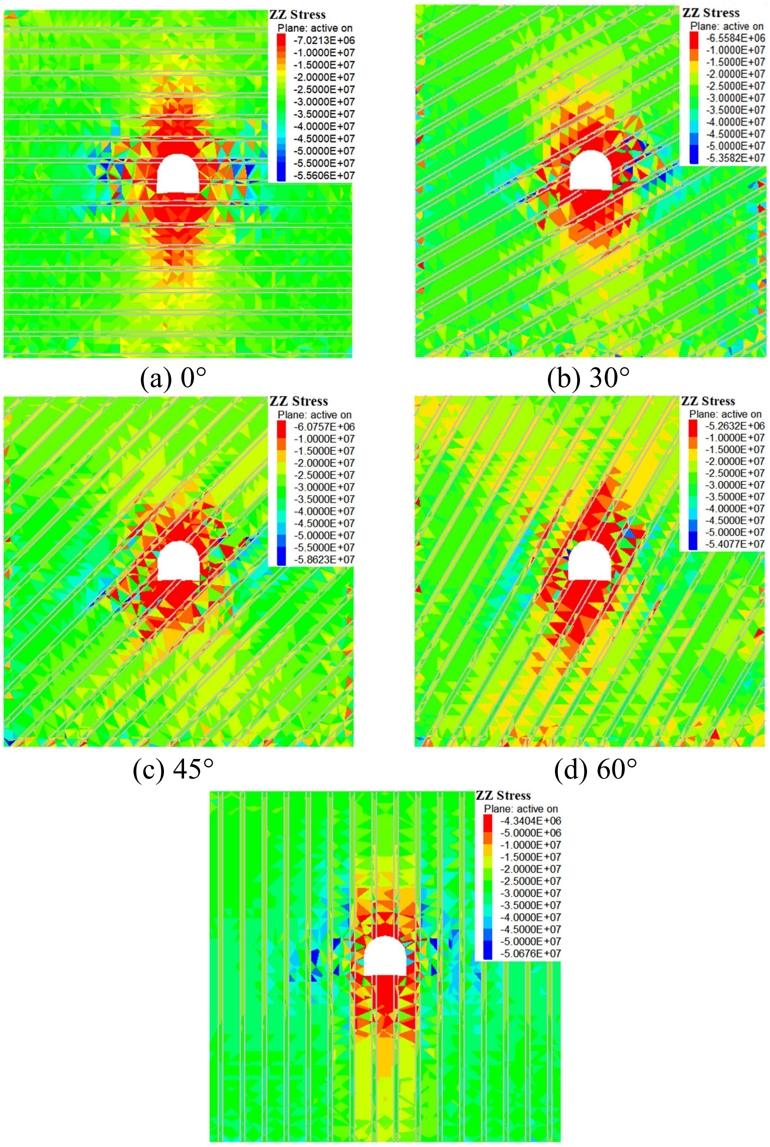

Figure 5. Vertical Stress Contours of the Surrounding Rock with Different Bedding Dip Angles (unit: Pa)

3.3 Plastic Zone Evolution

The evolution of the plastic zone in the surrounding rock is an important basis for evaluating tunnel stability and optimizing support schemes. The plastic zone distributions with different bedding dip angles are shown in Figure 6. It can be seen that the bedding dip angle has a significant influence on the plastic zone distribution in soft-hard interbedded surrounding rock. (1) The plastic zone mainly develops along the bedding planes, indicating that bedding discontinuities play a key role in controlling the failure propagation path of the surrounding rock. With increasing θ, the plastic zone exhibits an overall directional migration. On the right side of the tunnel, the plastic zone gradually shifts from the sidewall toward the arch foot, haunch, spandrel, and crown, whereas on the left side, it extends from the sidewall toward the wall foot and invert. (2) When θ = 0°, the plastic zones are mainly concentrated near the crown and invert, and the surrounding rock failure is primarily affected by tensile-shear failure along horizontal bedding planes. When θ = 30°~60°, the plastic zone expands markedly along the inclined bedding planes, and bedding-plane sliding becomes the dominant failure mode. When θ = 90°, the plastic zone is mainly developed around the sidewalls, indicating that local sidewall instability is more likely to occur under vertical bedding conditions. (3) Tunnel excavation disturbs the initial in-situ stress equilibrium and induces stress redistribution in the surrounding rock. When the local stress exceeds the strength of the rock mass or bedding discontinuities, plastic failure is first initiated along the bedding planes and stress concentration zones around the tunnel, and then gradually propagates outward. A comprehensive analysis of the plastic zone distribution indicates that θ affects not only the extent of plastic deformation in soft-hard interbedded surrounding rock, but also the propagation direction of the plastic zone and the potential instability locations.

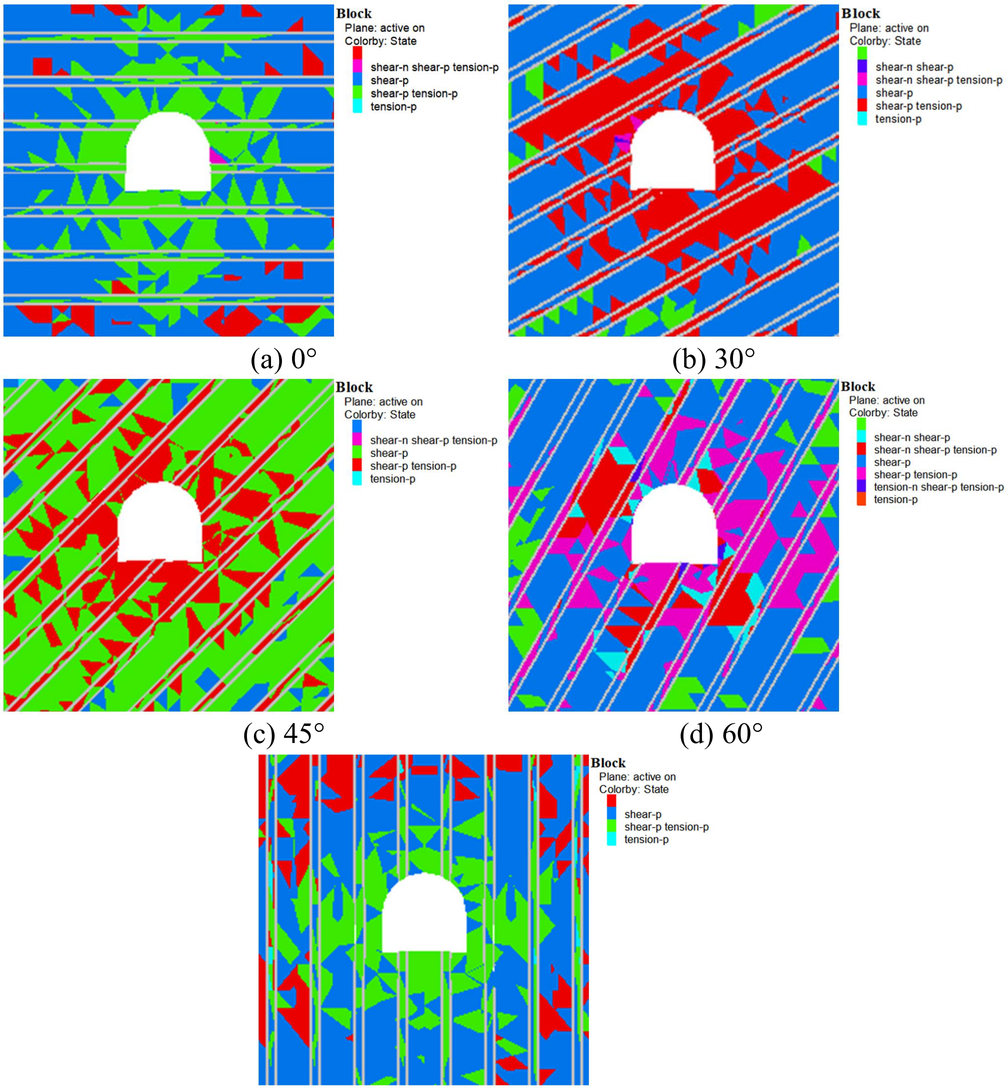

(a) 0° (b) 30°

(c) 45° (d) 60°

(e) 90°

Figure 6. Plastic Zone Distribution with Different Bedding Dip Angles

4. Conclusions

(1) The bedding dip angle exerts a pronounced influence on the vertical displacement response of the soft-hard interbedded surrounding rock. At θ = 0° and 90°, the vertical displacement field is generally symmetric. In contrast, for θ = 30°~60°, a distinct asymmetric pattern develops, with the high-value vertical displacement zones migrating along the bedding direction. This behavior indicates that inclined bedding interfaces intensify the asymmetric deformation of the interbedded rock mass. With increasing bedding dip angle, the overall magnitude of vertical displacement gradually decreases.

(2) The bedding dip angle has a pronounced controlling effect on vertical stress redistribution in the soft-hard interbedded surrounding rock. At θ = 0° and 90°, the vertical stress field is generally symmetric. In contrast, at θ = 30°~60°, the high vertical-stress zones migrate along the bedding direction, resulting in marked asymmetric stress concentration. As the bedding dip angle increases, the vertical stress in the surrounding rock exhibits an overall decreasing trend.

(3) The propagation of the plastic zone is significantly controlled by bedding discontinuities. With different bedding dip angles, the plastic zone in soft-hard interbedded surrounding rock mainly develops along the bedding planes. When θ = 0°, tensile-shear plastic zones are prone to form near the crown and invert. When θ = 30°~60°, bedding-plane sliding becomes the dominant mode of plastic zone propagation. When θ = 90°, the plastic zone is mainly developed around the sidewalls, indicating a higher risk of local sidewall instability.

Acknowledgments

This paper is supported by the Key Project of the Science and Technology Research and Development Program of China State Railway Group Co., Ltd. (No. N2024G049), the Natural Science Foundation of Henan Province (No. 252300420846) and the Key Scientific Research Projects for Higher Education of Henan Province (No. 26B620001).

References

[1] Shu Xiaoyun, Zhu zhende, Qu Shen, et al. Anisotropic Characteristics and Deformation Behaviors of Layered Rocks Surrounding Tunnel: A Review[J]. Journal of Rock Mechanics and Geotechnical Engineering, 2025, 17(12):8198-8223.

[2] Li Ang, Xu Nuwen, Dai Feng, et al. Stability Analysis and Failure Mechanism of the Steeply Inclined Bedded Rock Masses Surrounding a Large Underground Opening[J]. Tunnelling and Underground Space Technology, 2018, 77:45-58.

[3] Luo Yanbin, Chen Jianxun, Wang Libao, et al. Mechanical Model Calculations of Tunnel Roof with Horizontal StratifiedRock Mass Tunneling Considering the Interlayer Cohesion[J]. China Journal of Highway and Transport, 2018, 31(10):230-237+265

[4] Yan Bingqian, Wang Peitao, Ren Fenhua, et al. A Review of Mechanical Properties and Constitutive Theory of Rock Mass Anisotropy[J]. Arabian Journal of Geosciences, 2020, 13(12): 1-16.

[5] Zhao Jun, Li Changming, Huang Wei. Long-Term Anisotropic Mechanical Characterization of Layered Shale-An Experimental Study for the BaoKang Tunnel of the Zhengwan Railway, China[J]. Processes, 2025, 13(6).

[6] Zhang Wenju, Yang Qinghao. Influences of Bedding Planes Dip Angles on Creep Properties of Surrounding Rock and Mechanical Response of Tunnel Structure[J]. Construction Technology, 2019, 48(11):73-78.

[7] Li Lei, Tan Zhongsheng, Guo Xiaolong, et al. Large deformation of tunnels in steep dip strata of interbedding phyllite under high geostresses[J]. Chinese Journal of Rock Mechanics and Engineering, 2017, 36(07):1611-22.

[8] Ren Song, Ouyang Xun, Jiang Deyi, et al. Stability analysis and optimization of primary support on tunnel excavation with soft-hard interbed rock[J]. Journal of Huazhong University of Science and Technology (Natural Science Edition), 2017, 45(07):17-22.

[9] Tu Han. Research on the Stability and Failure Mechanism of Horizontal Layered Surrounding Rock Tunnel[J]. Journal of Railway Engineering Society, 2018, 35(09):75-9+87.

[10] Ding Yu, Chen Yong, Liu Xingxing, et al. Numerical Analysis of the Failure Law of Surrounding Rock in Sandstone Interbedded Tunnels with Different Dip Angles[J]. Chongqing Architecture, 2023, 22(07):12-4.

[11] Vitali Osvaldo P.M., Celestino Tarcisio B., Bobet Antonio. Behavior of tunnels excavated with dip and against dip [J]. Underground Space, 2021, 6(6):709-17.

[12] Huang Xinhui. Simulation Study on Surrounding Rock Deformation of Tunnels Crossing Hard-Soft Interbedded Strata[J]. Western China Communications Science & Technology, 2023, (07):116-9.